

From measurements to inferences of physical quantities in numerical simulations

Tota Nakamura

College of Engineering, Shibaura Institute of Technology, Saitama 337-8570, Japan

(Dated: October 15, 2018)

We propose a change of style for numerical estimations of physical quantities from measurements to inferences. We estimate the most probable quantities for all the parameter region simultaneously by using the raw data cooperatively. Estimations with higher precisions are made possible. We can obtain a physical quantity as a continuous function, which is differentiated to obtain another quantity. We applied the method to the Heisenberg spin-glass model in three dimensions. A dynamic correlation-length scaling analysis suggests that the spin-glass and the chiral-glass transitions occur at the same temperature with a common exponent ν . The value is consistent with the experimental results. We found that a size-crossover effect explains a spin-chirality separation problem.

Introduction- Estimations of physical quantities in numerical simulations are based on equilibrium statistical physics [1]. We virtualize a model system in a computer and perform *independent* measurements on the system using a definition of a physical quantity. When an evaluation process is complex, both systematic and statistical errors are accumulated in the obtained data. We sometimes encounter numerical instabilities, which may affect a final physical conclusion. In what follows, we explain the situation of interest using a correlation-length estimation.

An estimation formula for a correlation length, ξ , is given by the second-moment method: $\xi = \sqrt{\chi_0/\chi_k - 1/k}$ [2]. Here, χ_0 denotes the susceptibility and χ_k its Fourier transform with k as the lowest wave number of the system. This expression itself is problematic. Both numerator and denominator of this expression approach zero as the system size increases ($k \rightarrow 0$), where this formula becomes exact. We encounter the numerical instability caused by the expression $0/0$. In order to avoid this problem, Bellettiet *al.* [3] proposed the reduction of this instability by estimating ξ through the integrals $I_k = \int_0 drr^k f(r)$ and ξ is obtained as I_2/I_1 . Suwa and Todo [4] proposed a generalized moment method for gap ($\Delta \sim 1/\xi$) estimation in quantum systems. Systematic errors and ambiguity caused by using small- L data are eliminated.

Recently, big-data handling has become possible due to rapid increase in computational power. Data science is now one of the most promising fields in science and technology. As regards its application to physics, the topic of Bayesian inference has attracted considerable interest [5, 6]. In this context, Harada [7] introduced Bayesian inference into a parameter estimation of the finite-size scaling analysis.

In this paper, we extend its application to estimations of physical quantities. For example, we can obtain an analytic expression for an energy out of the discrete raw data as the most-probable model function. Then, we obtain the specific heat by analytically differentiating it. A critical temperature is estimated automatically within this procedure. Since directly-observed (raw) data are

cooperatively utilized in this inference procedure, we can reduce numerical errors and avoid numerical instabilities.

We also discuss in this paper a size crossover effect in random systems. Hukushima and Campbell [8] reported that there exists a crossover size, $L \sim 24$, where the finite-size effect of the correlation-length ratio, ξ/L , changes its trend from increasing to decreasing in the Ising spin-glass model. Similar non-monotonic size dependences have been observed in the $\pm J$ Heisenberg spin-glass model. The chiral-glass susceptibility of sizes smaller than $L = 39$ increases with the system size but that of larger sizes decreases [9]. Size-crossover effects were also observed in a random quantum spin chain [10, 11]. Short-range spin correlations exhibit an exponential decay, which suggests that the energy gap is finite; in contrast, the long-range ones exhibit an algebraic decay indicating that the energy gap is zero. The size-crossover effect may influence the final physical conclusion. We explain contradictory arguments on a spin-glass transition by this effect.

Method- We explain the method in a two-dimensional Ising ferromagnetic model. We performed equilibrium simulations and obtained data for energy, E_i , and the magnetization, M_i , at each temperature, T_i , where i is the data index. The linear system size is 999, and it is set to 1999 in the vicinity of the transition temperature. These data are depicted in Fig. 1 by circle symbols. We fit them by the Gaussian kernel regression [7, 12] using three variables, x_i , y_i , and ϵ_i defined as

$$\begin{aligned} x_i &= \ln |T_i - T_c| \\ y_i &= \ln(-E_i) \quad (y_i = \ln |M_i| \quad \text{for } M) \\ \epsilon_i &= (\delta E_i/E_i)^2 \quad (\epsilon_i = (\delta M_i/M_i)^2 \quad \text{for } M). \end{aligned}$$

Here, δE_i and δM_i denote errors for E and M , and T_c denotes the critical temperature that is to be estimated in the following analysis. We defined a Gaussian kernel function as $K(x_i, x_j) = \theta_0^2 \exp \left[-\frac{(x_i - x_j)^2}{2\theta_1^2} \right] + \theta_2^2$, where θ_0, θ_1 , and θ_2 are hyper parameters. A generalized covariance matrix is $\Sigma_{ij} = \epsilon_i \delta_{ij} + K(x_i, x_j)$. Then, the following log-likelihood function is to be maximized: $\ln \mathcal{L} = -\frac{1}{2} \ln |2\pi \Sigma| - \frac{1}{2} y_i \Sigma_{ij}^{-1} y_j$. This function is de-

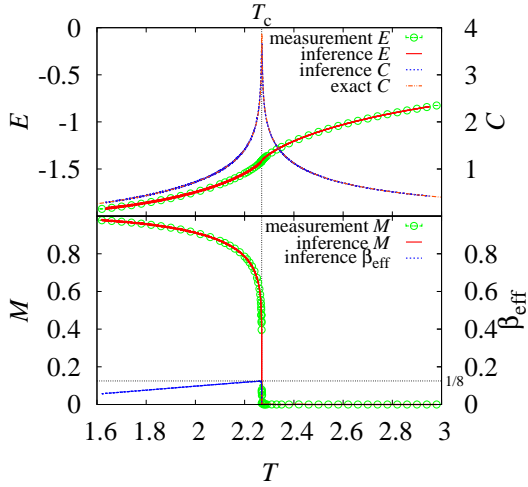


FIG. 1: (Color online) Temperature dependences of energy(E), magnetization(M), the specific heat(C), and the effective critical exponent β_{eff} in the two-dimensional Ising ferromagnetic model. Error bars are smaller than the symbols and line widths.

finely independently for both $T_i > T_c$ and $T_i < T_c$, and we take a summation of them. The hyper parameters, $\{\theta_0, \theta_1, \theta_2\}$, are also defined independently for two regions. We searched for seven parameters, one T_c and two sets of $\{\theta_0, \theta_1, \theta_2\}$, that maximizes the log-likelihood function by using the downhill simplex method [13]. We tried this search for four hundred times by changing the initial values of the parameters. We estimated averages and error bars for parameters over them. The critical temperature is obtained as a parameter that separates the data into two regions, where the data are fitted most smoothly. It was $T_c = 2.26914(4)$ for the E inference and $T_c = 2.26919(4)$ for the M inference. They are very close to the exact value $T_c = 2.269185314 \dots$. Using the obtained parameter set, we write a model expression for E as

$$E(T) = -\exp[K(x, x_i) \Sigma_{ij}^{-1} y_j], \quad x = \ln |T - T_c|, \quad (1)$$

where the summation over i and j are taken. We differentiate this function *analytically*, and we obtain the specific heat, $C(T) = \frac{dE}{dT}$, as a continuous function. The inference results for $E(T)$ and $C(T)$ are depicted by lines in Fig. 1. We confirmed that the $C(T)$ function is consistent with the exact results. We obtained a function for M in the same manner. Since $M \sim (T_c - T)^\beta$, the effective β is given by $\beta_{\text{eff}} = \frac{dy}{dx}$ with $y = \ln |M(T)|$. A critical exponent $\beta = 1/8$ is a value at $T = T_c$. A critical region, where β_{eff} approximately equals to $1/8$, is very narrow.

The nonequilibrium relaxation method [14–17] was proposed to treat large systems in a simple and easy manner. This approach has been applied successfully in random systems [9–11, 17–20]. The dynamic correlation-

length scaling method [21] was proposed as a variation of this method. We use this method together with the inference method to clarify the spin-chirality problem in the Heisenberg spin-glass model in three dimensions.

Model- A spin glass is a disordered magnet characterized by frustration and randomness [22, 23]. One of the most important and unsolved problems in spin-glass studies is the coupling or separation of the spin-glass (sg) degrees of freedom and chiral-glass (cg) degrees of freedom [18, 24–41]. Kawamura [25, 26] introduced the chirality scenario, wherein the cg order exists without the sg order. There is another scenario, in which the sg and cg transitions occur simultaneously. In 2009, two studies [38–40] on this topic drew two opposite conclusions even though the authors in each case performed similar amounts of simulations, but treated the finite-size effects differently. The present situation suggests that we need considerably larger system sizes to address this problem.

Our model Hamiltonian is: $\mathcal{H} = -\sum_{\langle i,j \rangle} J_{ij} S_i S_j$. The summation runs over all the nearest-neighbor spin pairs. The interactions J_{ij} take on two values, $\pm J$, with the same probability. The temperature T is scaled by J . The model is defined on a simple cubic lattice of the form $N = L \times L \times (L + 1)$ with $L = 159$. The skewed periodic boundary conditions were applied. We calculated the sg/cg susceptibility, $\chi_{\text{sg}}/\chi_{\text{cg}}$, sg/cg correlation functions, $f_{\text{sg}}/f_{\text{cg}}$, and sg/cg correlation length, $\xi_{\text{sg}}/\xi_{\text{cg}}$. One Monte Carlo (MC) step consists of one heat-bath update, 1/20 Metropolis updates (once every 20 steps), and 124 over-relaxation updates. All the random bond configurations are different at each temperature. A typical sample number at one temperature is 20. More samples are treated near and above the transition temperature. In the study, we ran simulations at 42 sets of temperatures, and the total sample numbers were 1168. We evaluated the order parameters using 435 overlaps among 30 real replicas. At some lower temperatures, we evaluated them using 1128 overlaps among 48 real replicas and checked for consistency regarding the replica number. In the nonequilibrium relaxation study on the spin glasses, the thermal average is replaced by the replica averages [21]. The replica number needs to be larger than the value in the equilibrium simulations. Numerical error bars were estimated in regard to the sample average.

Results- We prepared the relaxation data of correlation functions, $f(r, t)$ [r denotes distance and t the measuring time step], obtained in the conventional measurement scheme. Figure 2 shows the sg and cg correlation functions for typical time steps in the range from $t = 316$ to 79433. The temperature, $T = 0.200$, is close to the transition temperature. We also plot the small- L ($L = 39$) data at $T = 0.210$ as shown by circles. The inverse of the slope of the curve in this figure corresponds to the correlation length. Here, we found the crossover distance, r_c , dividing the short-range correlation region and the long-range correlation region. Short-range correlations

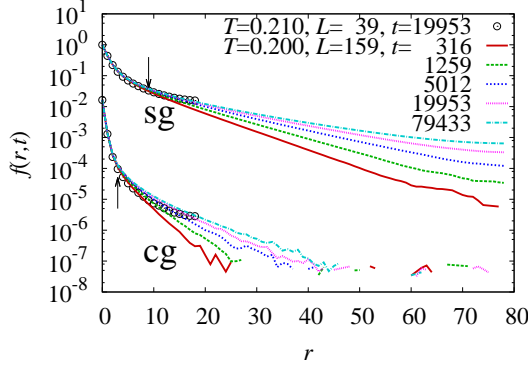


FIG. 2: (Color online) Correlation function data for selected time steps for $L = 39$ (circles) and $L = 159$ (lines). Arrows depict crossover distances between short-range correlations and long-range correlations ($r_c = 9$ for sg and $r_c = 3$ for cg).

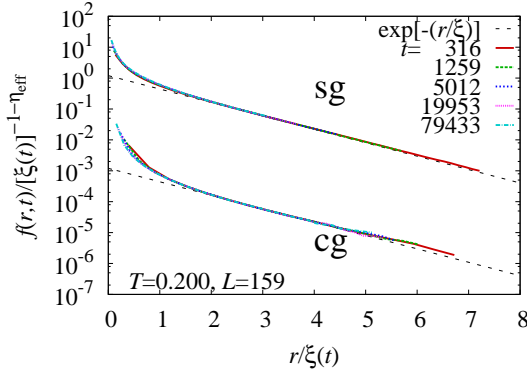


FIG. 3: (Color online) Scaled correlation function data for $r < L/3$.

do not depend on t , T , and L . Meaningful information is not included in this region. The growth of the correlation length is only reflected in the long-range correlations. The sg crossover distance ($r_c \simeq 9$) is roughly three times greater than the cg one ($r_c \simeq 3$). The effects of the periodic boundary conditions appear as the distance approaches $L/2$. We use only the data in the distance range of $2r_c < r < L/3$ to exclude influences of short-range correlations and the boundary effects.

The correlation lengths are related to the correlation functions via the following scaling ansatz:

$$f(r, t)/[\xi(t)]^{1-\eta_{\text{eff}}} = \mathcal{F}(r/\xi(t)), \quad (2)$$

where \mathcal{F} denotes the scaling function and η_{eff} is the effective scaling exponent. In a Gaussian kernel regression procedure, we set $x_i = r/\xi(t)$, $y_i = f(r, t)/[\xi(t)]^{1-\eta_{\text{eff}}}$, and $\epsilon_i = \delta y_i^2$, with i denoting an index number for all the combinations of (r, t) . We estimate $\xi(t)$ and η_{eff} as parameters so that all the $f(r, t)$ data fall onto a single scaling function \mathcal{F} . Dozens of $\xi(t)$ data sets are obtained simultaneously from thousands of $f(r, t)$ data sets. Consistency among many data sets yields accurate estimates

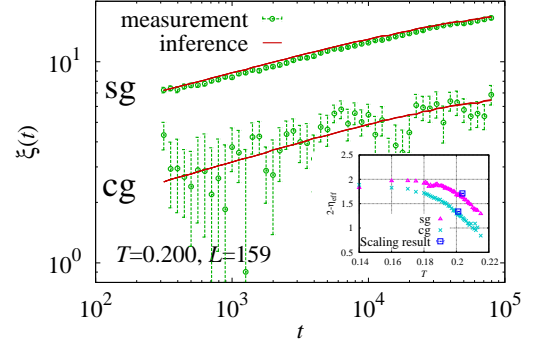


FIG. 4: (Color online) The correlation length data estimated by the inference and that by the measurements (the second-moment method). Error bars for the inference data are smaller than line widths. Inset: Temperature dependences of the effective exponent η_{eff} . The critical exponent η obtained by the dynamic correlation-length scaling analysis is also plotted.

of the correlation length.

Figure 3 shows the result of scaling. We rescaled $\xi(t)$ so that the slope of this plot becomes unity as $\mathcal{F}(r/\xi(t)) \sim \exp[-r/\xi(t)]$. This rescaling defines the unit of the length scale. Figure 4 shows the obtained $\xi(t)$. We compare our inference results with those obtained in the measurement scheme (the second-moment method). The sg data obtained with both methods show a close consistency. On the other hand, numerical instabilities are observed in the cg estimations by the measurement method. In contrast, the inference method solves this instability problem. The effective exponent, η_{eff} , depends on the temperature reflecting a correction to scaling. We plot the η_{eff} values in the inset of this figure. It coincides with the critical exponent at the transition temperature, which will be obtained by the scaling analysis.

We apply the dynamic correlation-length scaling analysis [21] using the obtained $(\xi(t), \chi(t))$ data sets. Figure 5 shows the scaling plot of the sg and cg transitions. We applied the β -scaling method proposed by Campbell *et al.* [42]. We estimated the scaling parameters by the Bayesian inference introduced by Harada [7]. There are 1187 data sets in this figure, and we chose 800 data sets randomly and estimated the scaling parameters for 100 times. We determined the average and the error bar over them. We also plot in the inset the scaling result using ξ obtained by the measurement method. While it is impossible to perform scaling analysis on the cg data in the measurement method, our inference method made it possible. Estimated transition temperatures and critical exponents are summarized in Table I. The critical temperatures are consistent with previous results. Our values of ν_{sg} and η_{sg} are also consistent with those of the canonical sg materials [43–45]. This evidence suggests that the Heisenberg spin-glass model explains the

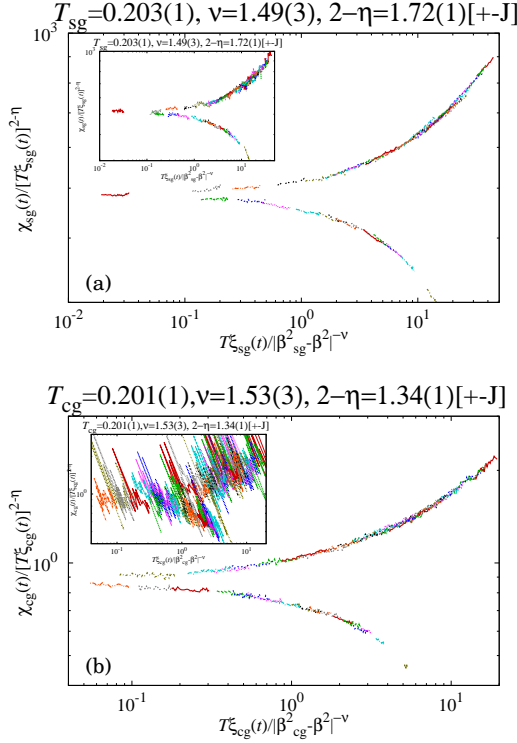


FIG. 5: (Color online) A scaling plot of (a) the sg transition and (b) the cg transition. Data of 42 sets of temperature ranging from 0.170 to 0.220 are depicted with different color lines. Insets depict the same scaling plot using the correlation length data obtained by the measurements (the second-moment method).

	T_{sg}	T_{cg}	ν_{sg}	ν_{cg}	η_{sg}	η_{cg}
this work	0.203(1)	0.201(1)	1.49(3)	1.53(3)	0.28(1)	0.66(1)
Ref-[18]	0.21(1)	0.22(1)	1.1(2)		0.27	
Ref-[35]	0	0.19(1)		1.3(2)		0.8(2)
Ref-[9]	0.203(1)	0.200(1)	1.79(2)	1.57(3)	0.19(1)	0.83(2)
Ref-[43]			1.40(16)		0.46(10)	
Ref-[44]			1.30(15)		0.4(1)	

TABLE I: Comparisons of our results with previous estimates. Refs-[43] and -[44] are experimental results of AgMn.

experiments.

Discussion and Summary—The evaluations of physical quantities in numerical studies are generalized to an inference scheme. This is a change of style in numerical investigations on statistical physics. We obtain the most-probable expression for a physical quantity from the discrete raw data. Then, we differentiate or integrate it analytically or numerically to obtain various quantities. We can improve accuracies of physical quantities because they are the product of consistency among many raw data sets. This method has potential applications not only to numerical studies on theoretical models but also to analyses on experimental data.

In our study on a Heisenberg sg model, we observed a simultaneous sg- and cg-transition with a common value of exponent ν . Here, one may ask why the sg- and cg-transitions have been observed sometimes differently and sometimes simultaneously. In what follows, we clarify this point. There are two important length scales when we discuss the finite-size effect. One is the correlation length and the other one is the crossover length. In the ferromagnetic Heisenberg model, the crossover length is only 2-3 lattice spacings. Thus, finite-size scaling analysis is possible using data with the minimum size $L = 6$ [46] or 8 [47]. As shown in Fig. 2, the sg crossover length is 9-10 lattice spacings in the Heisenberg spin-glass model. This value is comparable with the correlation length in the present simulation. The necessary length scale should be doubled or tripled under the periodic boundary conditions. This corresponds to a minimum lattice size $L = 20 - 30$. However, these sizes have been mostly the maximum sizes in the equilibrium simulations. On the other hand, the cg crossover length ($r_c = 2 - 3$) is almost same as that in the ferromagnetic model. The necessary size may be $L = 6 - 8$, which has been considered in the equilibrium simulations. This crossover-length issue is the reason why the sg transition was not detected in early simulations, while the cg transition was easily detected.

The author would like to thank Chisa Hotta, Naomichi Hatano, and Katsuyuki Fukutani for fruitful discussions. This work is supported by a Grant-in-Aid for Scientific Research from the Ministry of Education, Culture, Sports, Science and Technology, Japan (No. 24540413).

-
- [1] D. P. Landau and K. Binder, *A Guide to Monte Carlo Simulations in Statistical Physics* (Cambridge University Press, Cambridge, 2005), 2nd ed.
 - [2] F. Cooper, B. Freedman, and D. Preston, Nucl. Phys. B **210**, 210 (1989).
 - [3] F. Belletti, M. Cotallo, A. Cruz, L. A. Fernández, A. Gordillo-Guerrero, M. Guidetti, A. Maiorano, F. Mantovani, E. Marinari, V. Martin-Mayor, A. M. Sudupe, D. Navarro, G. Parisi, S. Perez-Gaviro, J. J. Ruiz-Lorenzo, S. F. Schifano, D. Sciretti, A. Tarancón, R. Tripiccione, J. L. Velasco, and D. Yllanes, Phys. Rev. Lett. **101**, 157201 (2008).
 - [4] H. Suwa and S. Todo, Phys. Rev. Lett. **115**, 080601 (2015).
 - [5] G. D’Agostini, Rep. Prog. Phys. **66**, 1383 (2003).
 - [6] U. Toussaint, Rev. Mod. Phys. **83**, 943 (2011).
 - [7] K. Harada, Phys. Rev. E **84**, 056704 (2011).
 - [8] K. Hukushima and I. A. Campbell, arXiv:0903.5026v1.
 - [9] T. Nakamura and T. Shirakura, J. Phys. Soc. Jpn. **84**, 013701 (2015).
 - [10] T. Nakamura, J. Phys. Soc. Jpn. **72**, 789 (2003).
 - [11] T. Nakamura, Phys. Rev. B **71**, 144401 (2005).
 - [12] C. M. Bishop, *Pattern Recognition and Machine Learning*

- (Springer, New York, 2006).
- [13] William H. Press, Brian P. Flannery, Saul A. Teukolsky, and William T. Vetterling, *Numerical Recipes in C* (Cambridge University Press, 1988).
 - [14] D. Stauffer, *Physica A* **186**, 197 (1992).
 - [15] N. Ito, *Physica A*, **192**, 604 (1993).
 - [16] Y. Ozeki and N. Ito, *J. Phys. A* **40**, R149 (2007).
 - [17] Y. Ozeki and N. Ito, *Phys. Rev. B* **64**, 024416 (2001).
 - [18] T. Nakamura and S. Endoh, *J. Phys. Soc. Jpn.* **71**, 2113 (2002).
 - [19] T. Yamamoto, T. Sugashima, and T. Nakamura, *Phys. Rev. B* **70**, 184417 (2004).
 - [20] T. Nakamura, S. Endoh, and T. Yamamoto, *J. Phys. A* **36**, 10 895 (2003).
 - [21] T. Nakamura, *Phys. Rev. B* **82**, 014427 (2010).
 - [22] *Spin Glasses and Random Fields*, ed. A. P. Young (World Scientific, Singapore, 1997).
 - [23] N. Kawashima and H. Rieger, in *Frustrated Spin Systems*, ed. H. T. Diep (World Scientific, Singapore, 2004).
 - [24] J. A. Olive, A. P. Young, and D. Sherrington, *Phys. Rev. B* **34**, 6341 (1986).
 - [25] H. Kawamura, *Phys. Rev. Lett.* **68**, 3785 (1992).
 - [26] H. Kawamura, *J. Phys. Soc. Jpn.* **79**, 011007 (2010).
 - [27] K. Hukushima and H. Kawamura, *Phys. Rev. E* **61**, R1008 (2000).
 - [28] F. Matsubara, S. Endoh, and T. Shirakura, *J. Phys. Soc. Jpn.* **69**, 1927 (2000).
 - [29] S. Endoh, F. Matsubara, and T. Shirakura, *J. Phys. Soc. Jpn.* **70**, 1543 (2001).
 - [30] F. Matsubara, T. Shirakura, and S. Endoh, *Phys. Rev. B* **64**, 092412 (2001).
 - [31] M. Matsumoto, K. Hukushima, and H. Takayama, *Phys. Rev. B* **66**, 104404 (2002).
 - [32] L. W. Lee and A. P. Young, *Phys. Rev. Lett.* **90**, 227203 (2003).
 - [33] L. Berthier and A. P. Young, *Phys. Rev. B* **69**, 184423 (2004).
 - [34] M. Picco and F. Ritort, *Phys. Rev. B* **71**, 100406(R) (2005).
 - [35] K. Hukushima and H. Kawamura, *Phys. Rev. B* **72**, 144416 (2005).
 - [36] I. Campos, M. Cotallo-Aban, V. Martin-Mayor, S. Perez-Gaviro, and A. Tarançon, *Phys. Rev. Lett.* **97**, 217204 (2006).
 - [37] L. W. Lee and A. P. Young, *Phys. Rev. B* **76**, 024405 (2007).
 - [38] L. A. Fernandez, V. Martin-Mayor, S. Perez-Gaviro, A. Tarancon, and A. P. Young, *Phys. Rev. B* **80**, 024422 (2009).
 - [39] D. X. Viet and H. Kawamura, *Phys. Rev. Lett.* **102**, 027202 (2009).
 - [40] D. X. Viet and H. Kawamura, *Phys. Rev. B* **80**, 064418 (2009).
 - [41] T. Shirakura and F. Matsubara, *J. Phys. Soc. Jpn.* **79**, 075001 (2010).
 - [42] I. A. Campbell, K. Hukushima, and H. Takayama, *Phys. Rev. Lett.* **97**, 117202 (2006).
 - [43] H. Bouchiat, *J. Phys. (Paris)* **47**, 71 (1986).
 - [44] L. P. Lévy, *Phys. Rev. B* **38**, 4963 (1988).
 - [45] I. A. Campbell and D. C. M. C. Petit, *J. Phys. Soc. Jpn.* **79**, 011006 (2010).
 - [46] P. Peczak, A. M. Ferrenberg, and D. P. Landau, *Phys. Rev. B* **43**, 6087 (1991).
 - [47] R. G. Brown and M. Ciftan, *Phys. Rev. Lett.* **76**, 1352 (1996).